

1 Abstract

Goal: Simple, fast, yet powerful local descriptor for gray-scale and rotation invariant texture classification.

- **Features:** Local pixel intensities and differences
→ easy to compute, complementary information
- **Feature space quantization:** Proposing CI-LBP, NI-LBP and RD-LBP via LBP-type of quantization
→ off-the-shelf textron codebook, low computational complexity, training free
- **Model:** Joint histogramming
→ simple, powerful
- **Classifier:** Nearest neighbor classifier
→ simple

2 Introduction

The welcome BoW model benefits from two complementary components:

- *local* discriminative and robust texture descriptors → a crucial factor in superior texture classification.
 - *global* statistical histogram characterization
- Motivations:
- To inherit the advantages of the BoW model
 - To enjoy the impressive computational efficiency of LBP
 - To avoid the limitations of LBP
 - To gain the benefits of combining complementary types of features

3 A Brief Review of LBP

Images are probed locally by sampling greyscale values at a central point $x_{0,0}$ and p points $x_{r,0}, \dots, x_{r,p-1}$ spaced equidistantly around a circle of radius r centered at $x_{0,0}$, as shown in Fig.1. Formally,

$$LBP_{p,r} = \sum_{n=0}^{p-1} s(x_{r,n} - x_{0,0})2^n, \quad s(x) = \begin{cases} 1, & x \geq 0 \\ 0, & x < 0 \end{cases} \quad (1)$$

An $N \times M$ image \mathbf{I} can be represented by a histogram vector \mathbf{h} of length $K = 2^p$.

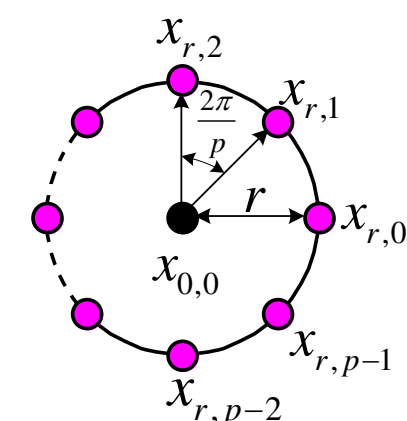
The conventional LBP has disadvantages

- the overwhelming dimensionality of \mathbf{h} with large p
- very sensitive to noise

Therefore, a better descriptor – the so-called ‘‘uniform’’ pattern $LBP_{p,r}^{riu2}$, has been proposed

$$LBP_{p,r}^{riu2} = \begin{cases} \sum_{n=0}^{p-1} s(x_{r,n} - x_{0,0}), & \text{if } U(LBP_{p,r}) \leq 2 \\ p+1, & \text{otherwise} \end{cases} \quad (2)$$

where $U(LBP_{p,r}) = \sum_{n=0}^{p-1} |s(x_{r,n} - x_{0,0}) - s(x_{r, \text{mod}(n+1,p)} - x_{0,0})|$.



4 Our Approach

We have proposed four descriptors (shown in Fig. 2) with the same form as the conventional LBP codes, thus they can be readily combined to form joint histograms to represent textured images.

1. NI-LBP:

$$NI - LBP_{p,r} = \sum_{n=0}^{p-1} s(x_{r,n} - \mu)2^n, \quad \mu = \frac{1}{p} \sum_{n=0}^{p-1} x_{r,n} \quad (3)$$

Similar to $LBP_{p,r}^{riu2}$, the rotation invariant version of $NI - LBP$, denoted by $NI - LBP_{p,r}^{riu2}$, can also be defined to achieve rotation invariant classification.

2. CI-LBP

$$CI - LBP = s(x_{0,0} - \mu_I) \quad (4)$$

relative to μ_I , the mean of image \mathbf{I} .

3. RD-LBP

$$RD - LBP_{p,r,\delta} = \sum_{n=0}^{p-1} s(\Delta_{\delta,n}^{\text{Rad}})2^n \quad (5)$$

4. AD-LBP

$$AD - LBP_{p,r,\delta} = \sum_{n=0}^{p-1} s(\Delta_{\delta,n}^{\text{Ang}})2^n \quad (6)$$

The proportions of the uniform patterns of AD-LBP were too small (Fig. 3) and inadequate to provide a reliable and meaningful description of texture images. Consequently we prefer not to include the AD-LBP in our experiments.

The samples are then classified according to their normalized histogram feature vectors \mathbf{h}_i and \mathbf{h}_j , using χ^2 distance metric

$$\chi^2(\mathbf{h}_i, \mathbf{h}_j) = \frac{1}{2} \sum_k \frac{[\mathbf{h}_i(k) - \mathbf{h}_j(k)]^2}{\mathbf{h}_i(k) + \mathbf{h}_j(k)}$$

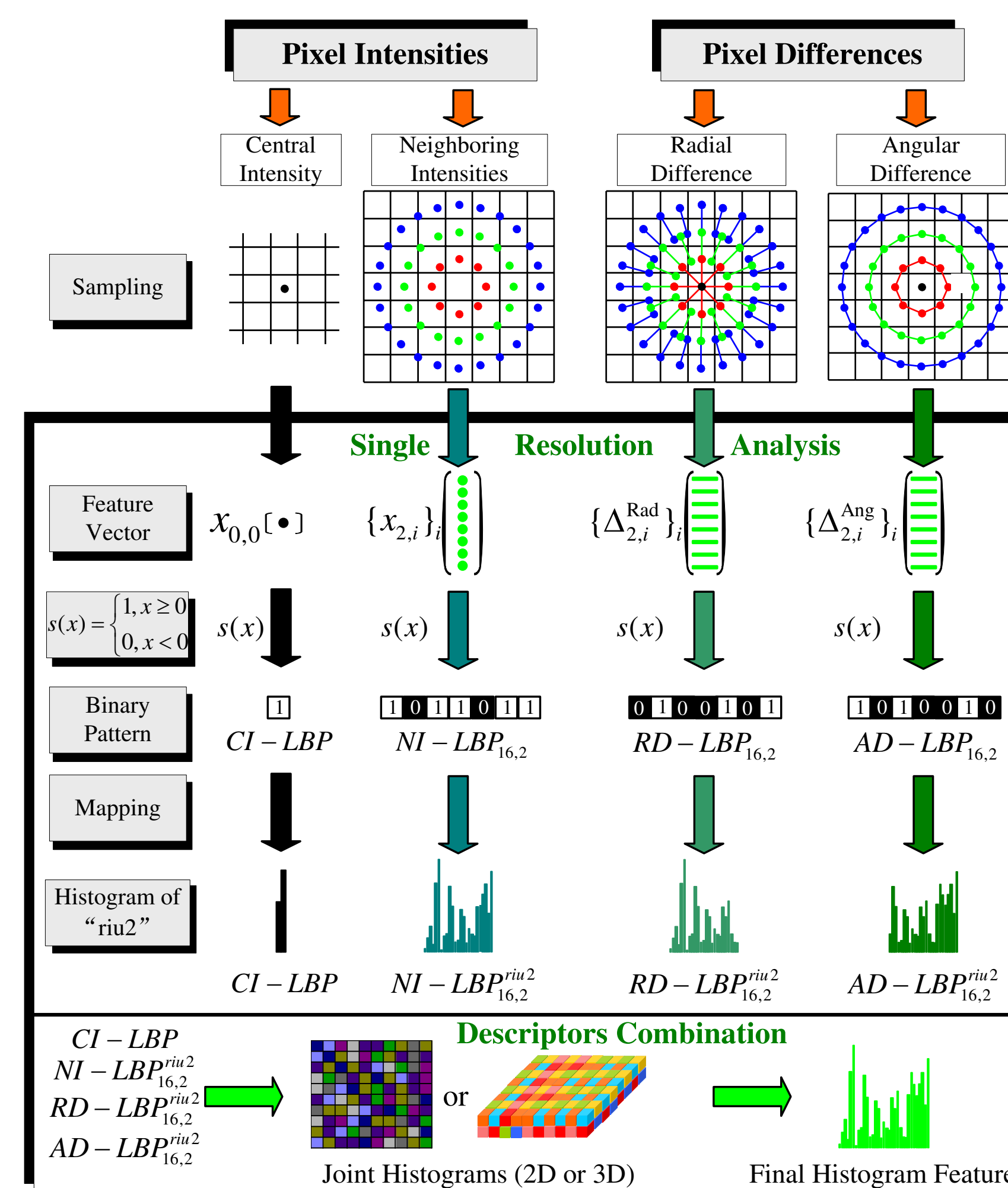


Fig. 2 Overview of the proposed approach

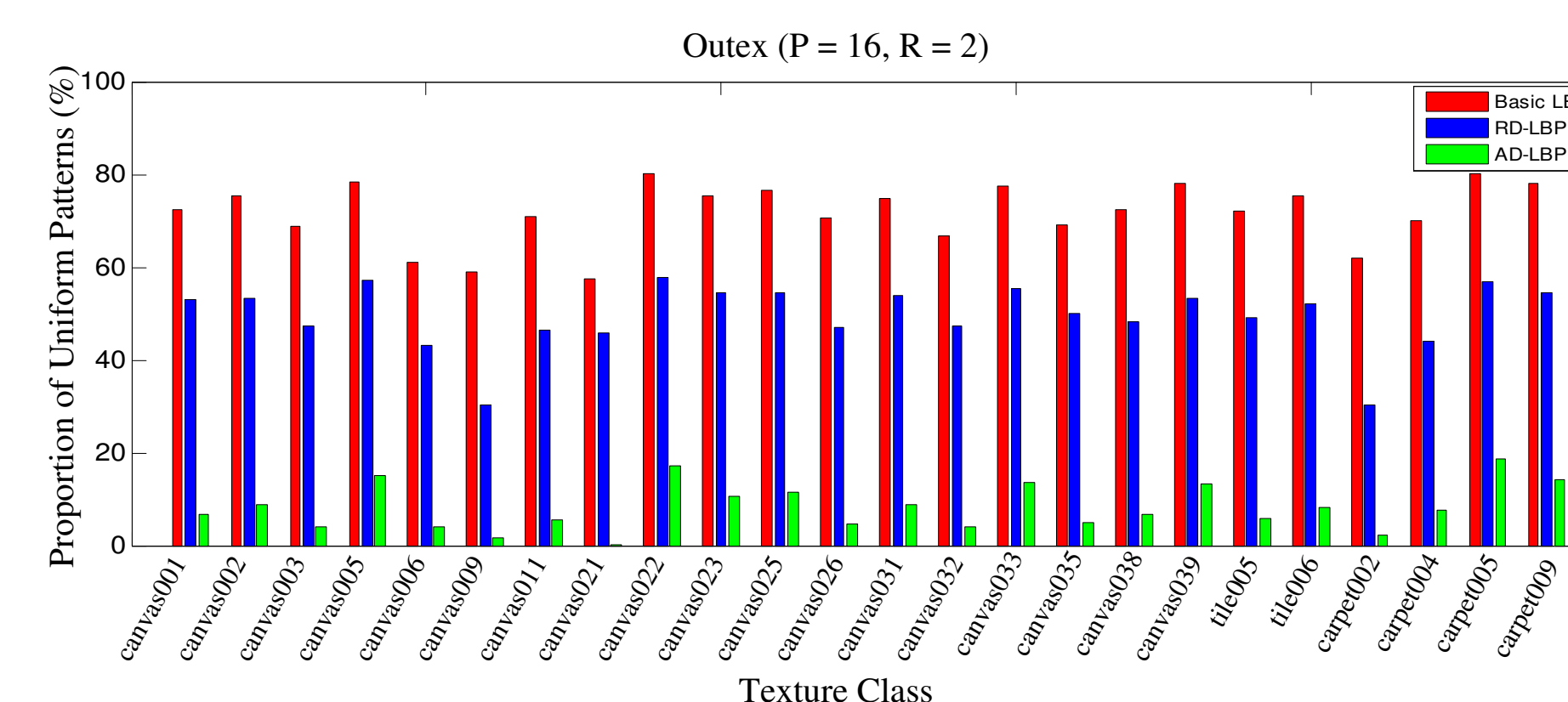


Fig. 3 Comparing the proportions (in %) of uniform patterns

5 Experimental Results

Table 1 Classification accuracies (%) on Contrib_TC_00001

Method	(p, r)	Bins	Rotation Angle for Train											Average								
			0°	20°	30°	45°	60°	70°	90°	120°	135°	150°										
LBP	(16,2)	18	96.2	99.0	98.6	98.9	98.5	99.1	97.6	98.6	98.7	97.5	98.3									
VAR	(16,2)	128	89.9	84.5	86.2	90.5	87.3	85.6	91.0	89.8	90.8	88.5	88.4									
LBP/VAR	(8,1)+(16,2)+(24,3)	864	100	99.7	99.5	99.8	99.6	99.7	99.8	99.6	99.8	99.9	99.7									
NI	(8,1)	10	65.4	85.5	81.3	76.6	77.0	78.4	68.8	81.4	75.8	76.5	76.7									
	(16,2)	18	87.6	95.2	92.3	93.6	89.4	96.0	88.9	91.3	93.4	90.1	91.8									
	(24,3)	26	96.2	93.4	97.6	96.6	98.3	96.7	97.1	96.7	92.6	98.2	96.4									
RD	(8,1)	10	68.8	86.4	84.4	76.0	84.9	84.4	70.2	84.1	76.1	84.7	80.0									
	(16,2)	18	89.2	92.9	96.7	97.8	96.1	92.6	88.4	94.7	96.7	97.3	94.3									
	(24,3)	26	87.6	90.6	98.2	90.8	96.5	93.8	89.5	98.6	89.5	94.2	92.9									
RD/CI	(8,1)	20	87.1	94.7	94.3	88.6	95.9	95.1	85.8	94.8	90.3	95.0	92.2									
	(16,2)	36	92.7	94.6	96.8	97.3	98.4	95.6	91.8	99.4	96.7	98.6	96.2									
	(24,3)	52	96.9	95.8	95.6	92.8	96.5	94.3	96.9	99.1	95.3	95.9	95.9									
NI/CI	(8,1)	20	74.8	90.4	86.4	80.3	82.5	85.2	74.4	86.2	80.6	82.2	82.3									
	(16,2)	36	95.6	99.2	98.8	98.0	98.2	99.4	93.8	98.3	96.9	97.4	97.6									
	(24,3)	52	99.1	98.7	99.4	99.4	100	100	99.7	97.5	97.3	99.1	99.1									
NI/RD	(8,1)	100	70.2	88.9	87.0	80.0	85.2	85.5	71.9	87.1	81.6	84.9	82.2									
	(16,2)	324	100	100	100	100	100	100	100	100	100	100	100									
	(24,3)	676	98.2	100	100	100	100	100	99.6	99.9	99.9	100	99.8									
NI/RD/CI	(8,1)	200	78.1	94.5	92.2	91.1	93.0	92.0	76.2	92.4	91.8	92.6	89.4									
	(16,2)	648	100	100	100	100	100	100	100	100	100	100	100									
	(24,3)	1352	98.8	100	100	100	100	100	99.8	100	99.8	100	99.8									

Table 2 Classification accuracies (%) for all the three Outex test suites

Test Suite	Outex_TC_00012			Outex_TC_00010			Mean Accuracy					
	‘‘t184’’	‘‘horizon’’	‘‘inca’’	(8, 1)	(16, 2)	(24, 3)	(8, 1)	(16, 2)	(24, 3)			
LBP	67.5	81.2	84.0	62.7	74.1	80.5	85.1	88.5	94.6	71.8	81.3	86.4
VAR	64.3	67.1	62.6	64.7	72.5	68.9	91.2	90.7	86.2	73.4	76.8	72.6
LBP/VAR	78.8	86.1	86.6	76.7	84.8	87.2	95.4	97.2	97.8	83.6	89.4	90.5
NI	59.1	71.9	76.3	56.2	65.5	72.2	76.4	87.0	88.7	63.9	74.8	79.1
RD	67.0	77.4	76.8	63.1	72.3	72.1	81.0	86.6	89.7	70.4	78.8	79.5
NI/CI	76.5	88.6	88.9	77.4	89.4	84.6	89.9	96.4	95.7	81.3	91.5	89.7
RD/CI	87.9	91.9	86.1	88.3	91.5	82.3	95.2	95.9	93.7	90.7	93.1	87.4
NI/RD	79.0	96.2	95.2	80.8	95.2	92.2	88.9	98.7	98.8	82.9	96.7	95.4
NI/RD/CI	90.9	98.0	97.3	92.7	98.0	96.2	96.5	99.3	99.2	93.4	98.4	97.6

Table 3 Classification accuracy (%) of descriptor NI/RD/CI for the three Outex test suites (training is done at just one rotation angle)

Test Suite	(p, r)	Rotation Angle for Train (‘‘inca’’)								Average	
		0°	5°	10°	15°	30°	45°	60°	75°		90°
Outex_TC_00012 (‘‘t184’’)	(8,1)	90.9	91.6	92.1	93.0	91.3	90.8	88.9	89.0	84.3	90.2
	(16,2)	98.0	98.3	99.1	98.6	98.4	98.6	98.6	98.6	97.7	98.3
	(24,3)	97.3	98.3	98.5	98.7	97.2	96.4	93.4	94.2	94.1	96.5
	(8,1)+(16,2)	97.4	98.0	98.4	98.5	98.3	98.3	97.8	97.1	95.6	97.7
	(8,1)+(24,3)	97.7	98.3	98.7	98.7	98.5	97.9	96.4	96.6	96.4	97.7
	(16,2)+(24,3)	98.3	99.0	99.3	99.2	98.9	98.9	98.3	98.1	98.1	98.7
Outex_TC_00012 (‘‘horizon’’)	(8,1)+(16,2)+(24,3)	98.5	98.9	99.1	99.1	99.0	98.9	98.4	98.2	98.1	98.7
	(8,1)	92.7	92.8	93.3	93.6	92.7	91.6	90.3	91.1	86.6	91.6
	(16,2)	98.0	98.0	98.3	98.4	97.7	97.9	98.2	98.3	98.1	98.1
	(24,3)	96.2	97.0	97.0	97.3	95.5	95.1	92.7	93.7	94.1	95.4
	(8,1)+(16,2)	98.2	97.8	98.3	97.9	97.1	97.8	98.2	97.8	97.0	97.8
	(8,1)+(24,3)	97.8	97.5	97.7	97.7	96.2	96.1	95.1	95.2	95.1	96.3
Outex_TC_00010 (‘‘inca’’)	(16,2)+(24,3)	97.8	98.3	98.2	98.3	97.3	97.5	96.9	97.0	97.7	97.7
	(8,1)+(16,2)+(24,3)	97.8	98.4	98.4	98.2	97.4	97.7	97.5	97.1	97.6	97.8
	(8,1)	96.5	96.3	97.4	97.6	96.2	95.3	92.7	94.9	91.8	95.4
	(16,2)	99.3	99.4	99.5	99.7	99.6	99.6	99.5	99.0	99.0	99.4
	(24,3)	99.2	99.5	99.4	99.5	99.5	99.5	99.2	99.3	99.1	99.4
	(8,1)+(16,2)	99.4	99.4	99.6	99.6	99.5	99.4	99.4	99.0	98.6	99.3
Outex_TC_00012 (‘‘horizon’’)	(8,1)+(24,3)	99.3	99.5	99.5	99.5	99.6	99.6	99.7	99.4	99.2	99.5
	(16,2)+(24,3)	99.6	99.7	99.8	99.7	99.7	99.9	99.8	99.7	99.5	99.7
	(8,1)	99.7	99.7	99.7	99.6	99.6	99.8	99.9	99.7	99.4	99.7
	(16,2)	99.3	99.4	99.5	99.7	99.6	99.6	99.5	99.0	99.0	99.4
	(24,3)	99.2	99.5	99.4	99.5	99.5	99.5	99.2	99.3	99.1	99.4
	(8,1)+(16,2)+(24,3)	99.7	99.7	99.7	99.6	99.6	99.8	99.9	99.7	99.4	99.7

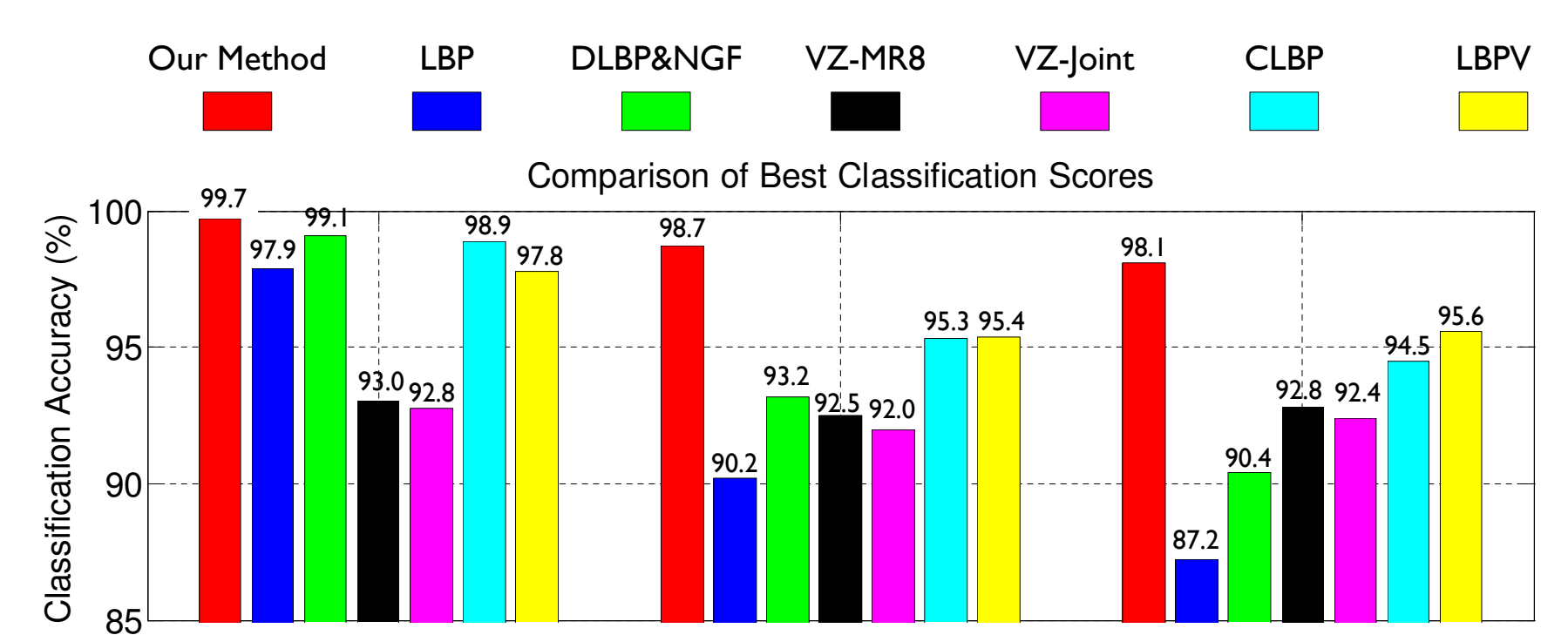


Fig. 4 Classification results (%) on Outex datasets: our method vs. state-of-the-art methods

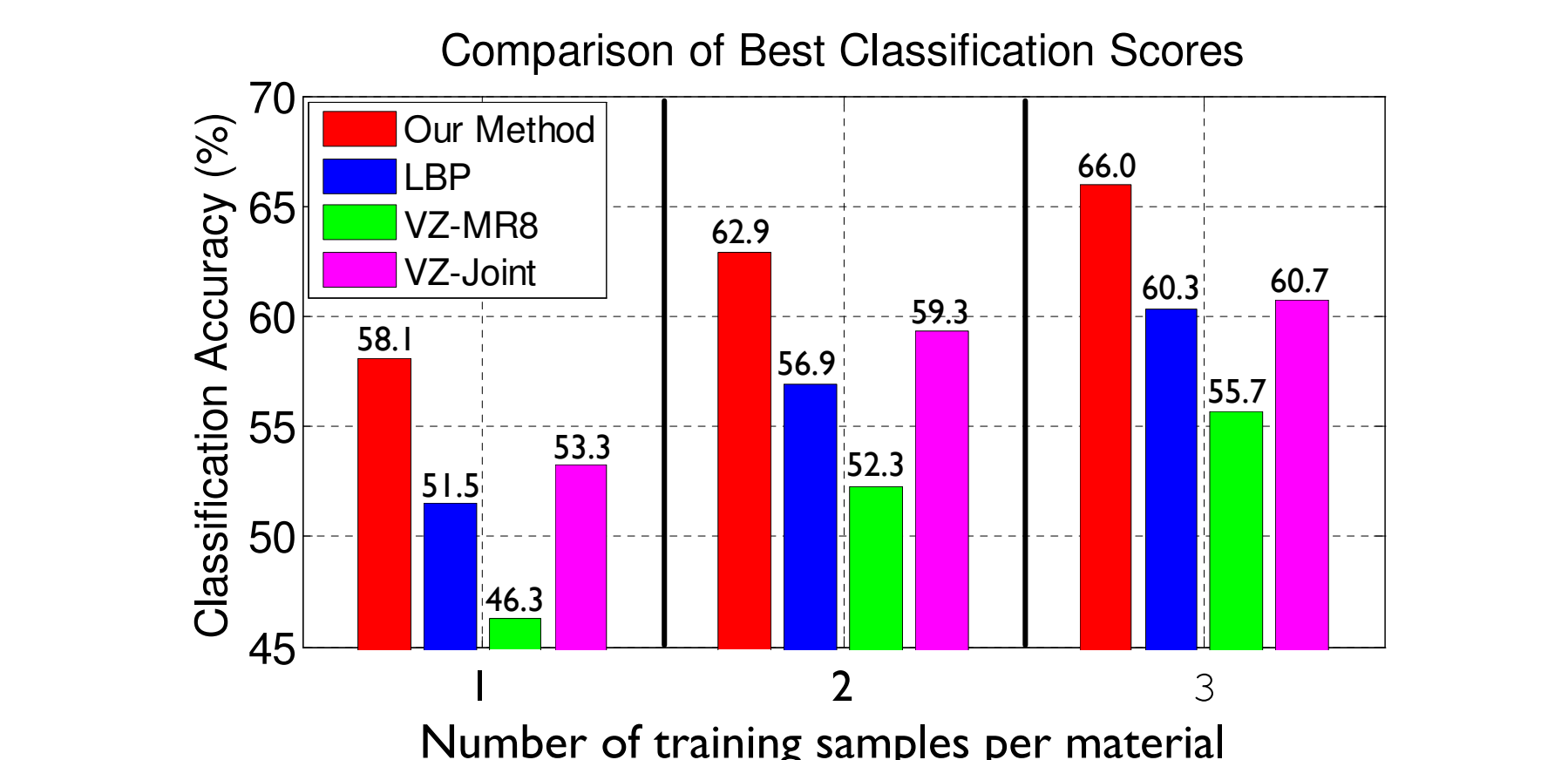


Fig. 5 Classification results (%) on KTH TIPS2b: our method vs. state-of-the-art methods